IEEE Access
Multidisciplinary | Rapid Review | Open Access Journal

Received 14 April 2023, accepted 1 May 2023, date of publication 8 May 2023, date of current version 17 May 2023.

Digital Object Identifier 10.1109/ACCESS.2023.3273777

RESEARCH ARTICLE

A New Approach for Estimation of Physical Properties of Irregular Shape Fruit

HIEU M. TRAN[1], KIEN T. PHAM[1], THANH M. VO[1], TAT-HIEN LE[2], TRI T. M. HUYNH[1], AND SON VU TRUONG DAO[3]

[1]School of Electrical Engineering, International University, Vietnam National University Ho Chi Minh City, Ho Chi Minh City 700000, Vietnam
[2]Faculty of Transportation Engineering, Ho Chi Minh City University of Technology (HCMUT), Vietnam National University Ho Chi Minh City, Ho Chi Minh City 700959, Vietnam
[3]School of Science, Engineering and Technology, RMIT University Vietnam, Ho Chi Minh City 700000, Vietnam

Corresponding author: Son Vu Truong Dao (son.daovutruong@rmit.edu.vn)

This work was supported by Vietnam National University Ho Chi Minh City (VNU-HCM) under Grant DN2022-20-02.

ABSTRACT Dimensions, volume, and mass of agricultural goods are essential physical features to build sizing, grading, and packaging systems. Manual property measurements are time-consuming, costly, and labor-intensive due to traditional technologies while various devices need to be installed to adapt process requirements. Furthermore, it is very challenging to accurately measure product with irregular or specific shapes, such as starfruit (Averrhoa carambola). Recently, there have been several research results on estimating features of the irregularly shaped object, they are either get inaccurate results or need repeated captures, computational resources, and time to rebuild the three-dimensional representation of the goods. The starfruit has not been studied completely in this size and weight measurements. This paper focuses on new techniques which exhibit simple installation to generate multiple functions for estimating the dimensions, volume, and mass with high accuracy. In this proposed method, we separated the process into two main phases. In the first phase, a camera is used to capture a top-view image of a starfruit, then image processing and machine vision techniques are applied to process the acquisition image before the process slices numerically the starfruit into several pieces along the longitudinal axis and estimates the physical attributes of each pieces using disc method and conical frustum method. Its volume is the summation of the volume of each partial slice. In the next phase, the density is used to estimate the mass of starfruit since the correlation coefficient (R-squared) between the volume and mass of starfruit is nearly linear with 0.9205. The validated results are highly competitive with accuracy of about 99% for the volume and mass in 300 testing samples.

INDEX TERMS Disc method, food measurement, food technology, frustum method, starfruit mass, starfruit volume.

I. INTRODUCTION

Starfruit (Averrhoa carambola), a nutritional and medicinal fruit is cultivated and consumed in tropical and many countries. In starfruit, there is a rich source of natural antioxidants and minerals [1], [2]. Furthermore, the import and export of starfruit increase worldwide. The United States of America imports starfruit at most with around $900 million in 2021 while the two top suppliers of starfruit are Canada and Thailand with nearly $500 and $400 million, respectively [3].

Due to its irregular shape, starfruit is hard for the production line to estimate the size, volume, mass, and other parameters when compared to other popular fruits with nice shapes. These parameters are major factors for setting up standards in the production line for packaging, conveying, grading, classifying, or processing. This makes the researchers investigate the physical characteristics of specific objects to find the best-fit design to speed up the process of production as Dang et al. [4] had researched a study of the geometric shapes parameters' performance contributions to the weight estimation procedure for mangoes then Dao et al. [5] had developed the artificial neural network for mass estimation

The associate editor coordinating the review of this manuscript and approving it for publication was Sunil Karamchandani.

of mangoes based on its visual information and extract the external quality parameters to grade, sort and classify mangoes. Mendoza et al. [6] also implemented computer vision techniques to identify a banana's ripening stages based on its color with 98% of accuracy. Other publications considered the shape varieties of fruits such as melon [7] to measure the mechanical properties or to find geometrical attributes of kiwi fruit [8], [9] to estimate its mass and volume. Previous research also investigated the characteristics, physical properties, surface area, etc. of other types of fruits such as strawberries [10], Thai coconut [11], apple [12], and sweet onions [13] by using image processing and machine vision techniques. In this study, we proposed an integrated system that includes multiple functions such as estimations of geometrical attributes, volume, and mass of starfruit. The physical attributes are measured by computer vision or image processing techniques, then the mass is estimated by linearity function of mass and volume which is pointed out in (1).

$$M = Vd. \tag{1}$$

where M is the mass (mg), V is the volume (mm^3), and d is the density (mg/mm^3).

Although traditional techniques such as Water Displacement Method (WDM) and Gas Displacement Method (GDM) are popular and have high accuracy in measuring volume, when we apply these methods to estimate fruit volume for the production line, there are many drawbacks, the objects will be harmed by the immersion into the liquid while using the water displacement method (WDM) or it needs a long time to process the gas displacement method (GDM). In recent years, three-dimensional shape determinations using cameras and ultrasonic devices, or X-rays, or projections of structured lights are potential ways to get a high-quality result for measuring the volume of objects. However, the cost for this installation outweighs the profit of the business and the system must be calibrated periodically. Moreover, this 3-Dimentions shape determinations method is applicable to use in the laboratory only because we need to work many times with many different angles to find the best solution, it also requires complicated algorithms to preprocess and reconstruct the object's 3D representation, which means the hardware needs to be strong enough to complete the workload in real time situation [14], [15], [16], [17], [18], [19], [20]. Therefore, this method not only takes a long time but also unsuitable for some low-cost production lines. There were some researchers estimated the volume of fruit using image processing techniques such as Miller et al. [21] determined the orange's volume by using its average diameter collected from 8 captured images at equal angular intervals and mathematic equations. Tillet et al. [22] used two cameras to get 12 different images of potatoes rolled along the conveyor belt and based on the related density among potatoes and the weight of each potato to estimate the volume. Forbes and Tattersfield [23] used image processing to estimate symmetrical fruit rotated around the x-axis to estimate the volume of the apple. In later years, Soltani et al. [24] based on the first Papus theorem to develop a mathematic model to estimate the volume of a banana without any image processing techniques, it was all about the elliptical cross-section. After that, image processing techniques were developed for axi-symmetric fruit to calculate the volume and surface area of objects, some researchers can be listed are Sabilov et al. [24], Wang and Nguang [25], and Khojastehnazhand et al. [26]. Md. Iqbal et al. [27] started to apply single-view images and a shape-based analytical model to estimate the volume of apple fruits. It analyzed five images taken by a digital camera and implemented the average result to increase the accuracy, then they extended it to the axi-symmetric fruit cases such as orange or lemon and decreased the deviation in volume estimation by using the specific case of the spherical, paraboloid, and ellipsoid with the appropriate analytic model to categorize fruits. Finally, they estimated the mass of fruits based on its density which is the relationship between volume and mass.

More recently, to increase the accuracy, various research got good results while focused on estimating volume using 3-Dimensions reconstruction [14], [16], [18] or Disc method [28], [29], [30] which sliced the fruit into many discs to get diameters, the height of each slice and find the sum of these slices to estimate the volume, or in 2018, Oyefeso et al. [31] measured sweet and Irish potatoes' volume and mass using geometrical attributes and get the highest R-Squared for sweet potato around 0.981 and R-Squared is equal to 0.968 for Irish potato, but when applying these methods to irregular shapes such as starfruit, it does not work effectively.

Regarding the mass estimation aspect, the digital scale is a popular way to weigh the fruit for some small-scale production lines and the strain gauge load cell [32], [33] is the most efficient way in large-scale production lines. For more detail, the strain gauge load cells transform the change in resistance to electrical signals, which is then filtered before being transformed to an analog value and passed to the analog-to-digital converter to determine the weight of the products. However, other parameters like temperature, humidity, or materials might affect the result of the load cell, so we need to re-calibrate it after a period of usage time unless the accuracy of the mass estimation will be decreased. Some companies are famous in this field such as A&D Inspection or Mettler Toledo, while the former company reveals a Checkweigher with the newest technology which can measure up to 320 packs per minute, the latter company released a combination of load cell and conveyor belt that can measure around 250 packs per minute [34], [35]. Especially, these methods can be used as their unique function, which means we need to install multiple methods for multiple purposes. Therefore, we need to implement and install many devices to complete a process. So, computer vision techniques are suitable directions to resolve these above disadvantages. Our proposed computer vision method just needs only one camera to take a single top view of a starfruit to estimate multiple parameters such as its volume, mass, grade, height, width, etc., with high accuracy and ease of installation. The rest of

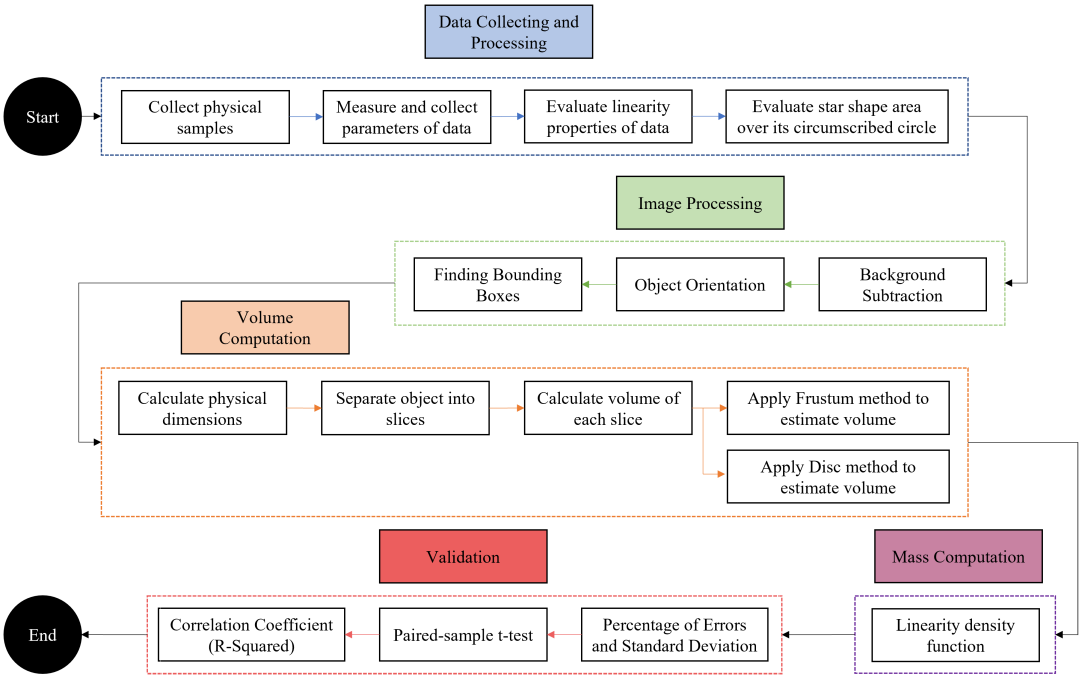

FIGURE 1. Process workflow of proposed method.

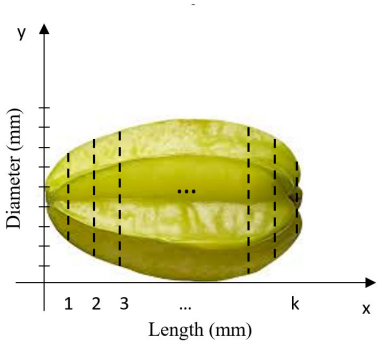

FIGURE 2. Slicing object into multiple pieces to estimate the volume.

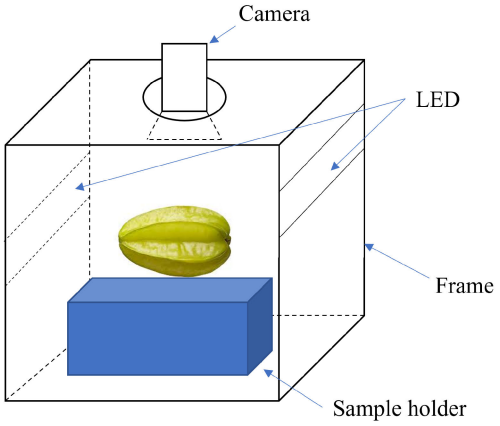

FIGURE 3. Hardware setup for taking top-view images of starfruit.

paper is structured as follow. Section II provides an overview of our materials, methods. Our experimental evaluations, results, discussions and validations are shown in Section III and the conclusion are mentioned in Section IV.

II. MATERIALS AND METHODS

The total step-by-step process in estimating the volume and mass of starfruit is shown in Figure 1. The measurement process starts to collect the data and analyze the linear properties between the mass and volume of starfruit then using the shape to find its physical properties. The process helps measuring the contour of the fruit and orienting it along a certain axis. Furthermore, the process includes manually measuring the ratio of the star shape area over its circumscribed circular area to determine the percentage of the area of each starfruit over its circumscribed circle.

Then, the starfruit is sliced into multiple pieces as shown in Figure 2. to calculate the volume of each piece and totalize volume of all slices to estimate the object's volume and calculate the mass based on its linearity density properties. Finally, the results will be validated by checking the percentage of errors, standard deviation [36], and correlation coefficient between actual and estimated data [36]. The paired-sample t-test is also applied to evaluate the difference between the means of our results to the means of reference volume, and mass.

A. HARDWARE SETUP

Our proposed hardware includes an aluminum chamber and a digital camera (CANON EOS 60D with lens Tamron 17-50, F2.8) which is put on top of the frame to capture the top perspective of object (Figure 3). To eliminate shadows and noise, two encircling LED light tubes are implanted inside.

FIGURE 4. Measurement tools which follow Tri T. M. Huynh, et al. [36].

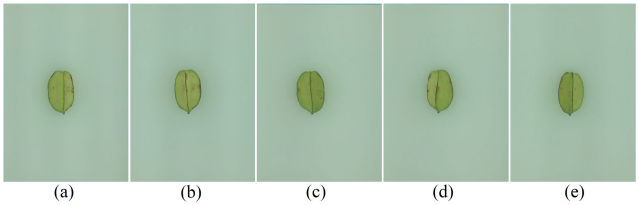

FIGURE 5. Each side of a starfruit are captured to validate the accuracy of algorithm.

Samples in this chamber are initially taken by the camera, and the system will calibrate the pixel square to estimate the volume, mass, and dimension. Furthermore, this study mainly uses Python programming language and OpenCV library to process the image, these methods are run on a laptop configured with CPU INTEL CORE I7 (10th generation) and 16GB RAM.

B. COLLECTING DATA FROM SAMPLES

1) MANUALLY COLLECT PHYSICAL DATA FROM SAMPLES

In the collecting data from samples procedure, three hundred starfruits with same variety (Averrhoa carambola L.), degree of ripeness (pale green in color) and various shapes were randomly collected from supermarkets in Ho Chi Minh City and were manually marked with an ordinal number, dimensions, mass, and volume for each object. These parameters are measured by standard laboratory methods to collect real data to compare with result of proposed method, particularly using a digital caliper (with an accuracy $\pm$ 0.1mm) to measure dimensions, using an electronic digital scale (with an accuracy of 0.1 g and can measure up to 3 kg) to measure the mass and implementing water displacement method (WDM) to measure the volume, this WDM method also gets the good accuracy due to the study of Chalidabhongse et al [20]. These tools (Digital caliper, Digital scale, Water displacement approach) are shown in order in Figure 4, respectively.

2) EVALUATE THE STAR SHAPE AREA OVER ITS CIRCUMSCRIBED CIRCLE

In this study, five images are captured for the five edges of each starfruit (as shown in Figure 5a-e) to validate the accuracy. Since the starfruit's specific shape and its five edges do not have the same width, our result will show the average of 5 estimated volumes for each starfruit based on

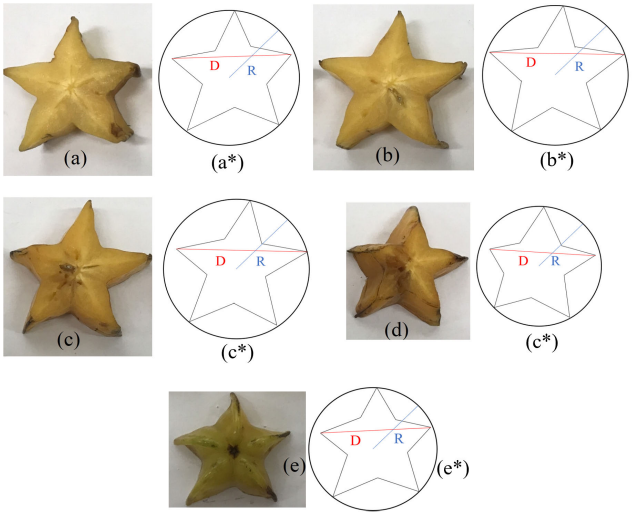

FIGURE 6. An example of 5 slices of a starfruit after slicing and their circumscribed radius R and diameters D based on its slice.

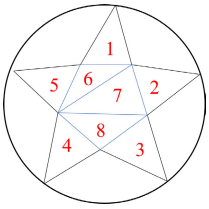

FIGURE 7. Star shape area separation.

their 5 sides and then display it as the average error and its average standard deviation in the result section.

Our method manually sliced 300 samples to around 1500 slices (with average 5 slices for each starfruit) to calculate the percentage of the area of each star shape area over the area of its circumscribed circle. Firstly, a starfruit was sliced into several pieces as shown in Figure 6a-e. Then, we find the best fit for the radius of circumscribed circles based on its relationship with the diameter (straight line connecting 2 non-adjacent points) which is shown in (2) where R is the radius of circumscribed circle and D is the diameter and presented in Figure 6a*-e*.

$$R = \frac{Dsin^{-1}(\pi/5)}{(1+\sqrt{5})} \tag{2}$$

After that, the area of the star shape of each slice is calculated by a sum of eight triangle areas which are shown in Figure 7, while each triangle area is calculated by Heron [37], which is shown in (3).

$$S_{ss} = \sum_{i=1}^{8} S_i = \sum_{i=1}^{8} \sqrt{p(p-e_{ia})(p-e_{ib})(p-e_{ic})} \tag{3}$$

where S_{ss} as the area of the star shape of each slice which includes 8 inside triangles (S_i), e_{ia}, e_{ib}, e_{ic} are three edges of the triangle i (S_i) and p $= (e_{ia} + e_{ib} + e_{ic})/3$. The percentage of the star shape area over the circumscribed circle is linear

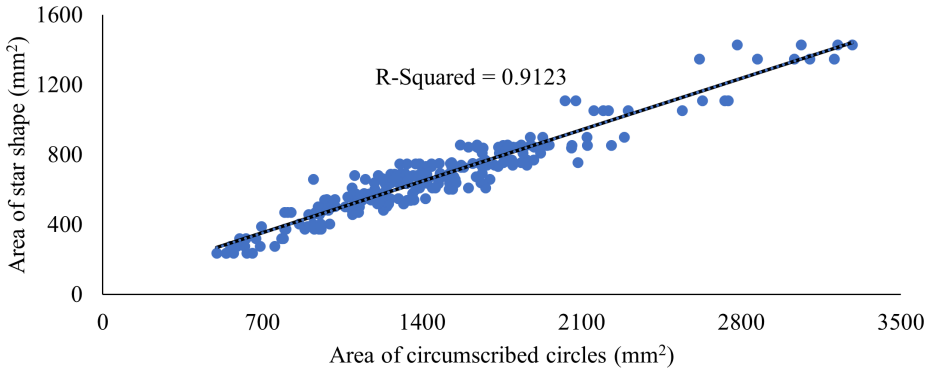

FIGURE 8. The correlation coefficient between the star shape area and its circumscribed circle area.

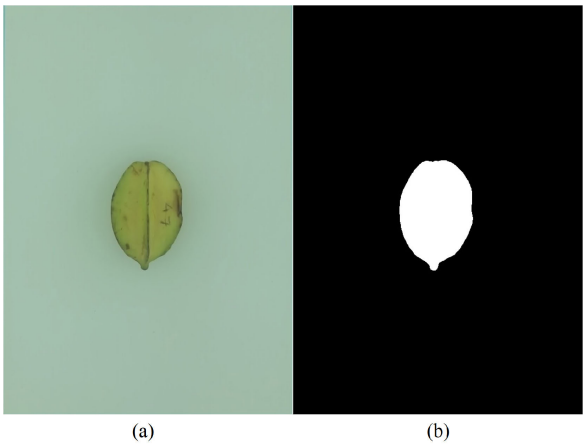

FIGURE 9. Original Input (a) and Image after applying background subtraction binarization process (b).

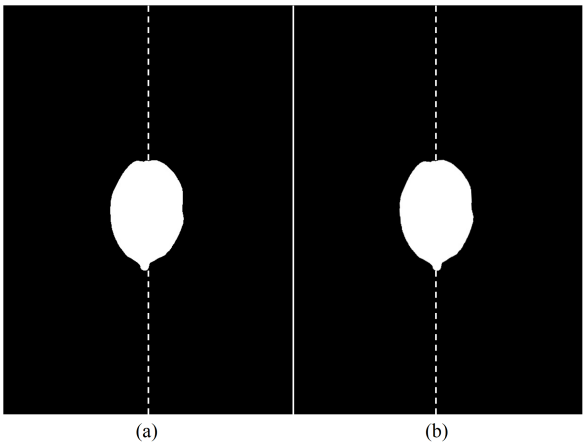

FIGURE 10. Before (a) and after (b) applying Object Orientation step.

(shown in Figure 8) and is the average value of the circumscribed cross-section minus the part that does not include the cross-sectional area of starfruit. This average percentage is found statistically around 42% and is calculated by (4).

$$\alpha = \frac{S_{ss}}{\pi R^2} \tag{4}$$

where α is the ratio between the star shape area over the area of its circumscribed circle, R is the radius of the circumscribed circle. This α plays a vital role as a constant in (9) and (10) which equals 0.42 (42%).

C. IMAGE PROCESSING

In the image processing section, we applied background subtraction, orientation object and finding bounding boxes techniques to the input image.

1) BACKGROUND SUBTRACTION

In this study, we decided to use OpenCV libraries to process RAW input images with the 2100 × 2970 (pixels) resolution as A4 paper size for easy calibrating.

Firstly, an image is converted to a grayscale image, then apply Gaussian Blur method to blur the input image After that, we apply binary thresholding and adaptive thresholding (Otsu's method) to make the object cleaner and find the suitable parameter to remove noise. The input image and the image after applying the background subtraction process are shown in Figure 9.

2) OBJECT ORIENTATION

Since the significant and irregular shape of starfruit and it is easier to apply the Disc and Frustum method which will be mentioned in the next section, the image must be orientated so that the fruit's stem-calyx axis is parallel to the image's vertical or horizontal edge to avoid the increasing error when applying our algorithm which shown in Figure 10.

The angle of inclination or angle of tilt of the stem-calyx axis should be calculated from the fruit border pixel data using the following approach [27]. Considering (x_i, y_i) for $i = \{1, 2 \ldots n\}$ as the set of boundary pixel points, the angle of tilt ϕ, with respect to horizontal axis can be determined as:

$$\phi = (0.5)tan^{-1}(2I_{XY}/(I_X - I_Y) \tag{5}$$

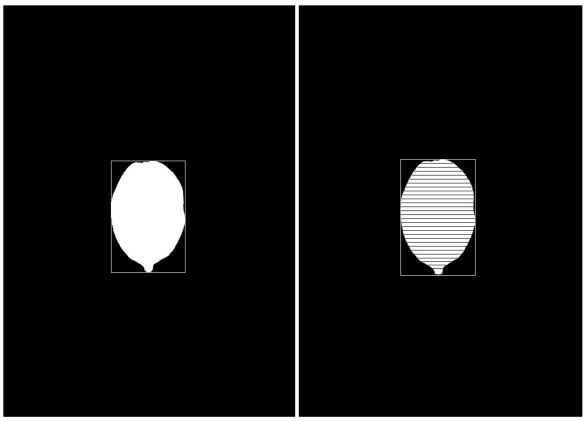

FIGURE 11. Bounding box (a) and an example of slicing a starfruit into 30 equal pieces (b).

where

$$I_X = \sum_{i=1}^{n}(x_i - x_{av})^2, I_Y = \sum_{i=1}^{n}(y_i - y_{av})^2 \tag{6}$$

$$I_{XY} = \sum_{i=1}^{n}(x_i - x_{av})(y_i - y_{av}) \tag{7}$$

and

$$x_{av} = \sum \frac{x_i}{n}, y_{av} = \sum \frac{y_i}{n} \tag{8}$$

I_X and I_Y are moment of inertia about x-axis and y-axis, respectively, I_{XY} is the product of inertia, x_{av} and y_{av} are the average values of the x-coordinates and y-coordinates of n pixel points in the contour and n is the number of boundaries pixel points.

3) ORIENTATION BOUNDING BOXES

After receiving the output from the object orientation process, the Canny edge detection and finding contours algorithm are implemented to find the maximum white area on an image and then get its location information (4-corner position) to create the biggest bounding box (white rectangle in Figure 11). Now, we can get some physical parameters of the starfruit such as the width and height by counting pixels after the calibration steps.

D. VOLUME COMPUTATION

Our proposed program was developed with the assumption that all objects have axisymmetric geometry, defined as a circular cross-section at any location perpendicular to the vertical axis, and utilizes the ratio of star shape area over its circumscribed circle to estimate the volume of starfruit. During the image capture procedure, the axi-symmetric object was digitized into tiny image elements or pixels. The image was represented after digitalization by a series of simple cylindrical objects 1 pixel in height which will be calibrated into millimeters in a later step.

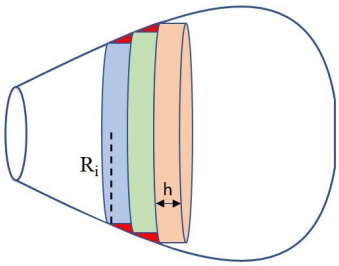

FIGURE 12. Disc Method.

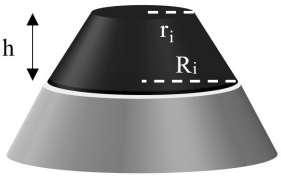

FIGURE 13. Frustum Method.

1) DISC METHOD

The Disc method is a method for estimating the volume of solids of revolution. It may be used for two-dimensional rotated objects with the axis of rotation also serving as the boundary (edge) and cross sections (thin slices) perpendicular to the axis of rotation. The sample's volume and surface area may be determined by combining the partial areas and volumes of individual cylinders which are shown in Figure 12.

$$V_{total(Disc)} = \sum_{i=1}^{n} V_i = \pi h \alpha \sum_{i=1}^{n} R_i^2 \tag{9}$$

where α is the ratio of star shape area over circumscribed circle which is mentioned in (4), h is disc height, and R_i is disc radius.

2) FRUSTUM METHOD

Since the main technique of this algorithm is summing the volume of the cylinder, the remaining space (the red region in Figure 12) between the edge and these cylinders cannot be accounted for, and a sizable inaccuracy in the estimate will increase through the length of the starfruit. So, cylinders are combined with elementary frustums of right circular cones to resemble better the form of the object which is shown in Figure 13. The object's volume was determined as the sum of the volumes of the partial cones, as shown below.

$$V_{total(Frustum)} = \sum_{i=1}^{n} V_i = \frac{\pi h \alpha}{3} \sum_{i=1}^{n} R_i^2 + r_i^2 + R_i r_i \tag{10}$$

where α is the ratio of star shape area over circumscribed circle, h is frustum height, R_i is frustum bottom radius and r_i is frustum top radius.

E. MASS COMPUTATION

The linear property of density (mg/mm^3) of 300 training starfruit samples are presented in Figure 14 with the R-Squared

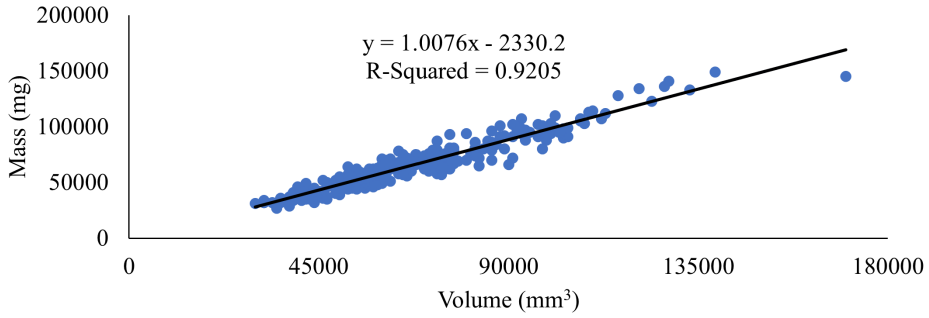

FIGURE 14. Density of starfruit samples.

TABLE 1. Statistical properties of 300 starfruit samples.

Descriptive statistic	Actual	
	Volume (mm^3)	Mass (mg)
Min	31,000	28,000
Max	78,000	68,000
Mean	49,500	44,800
Std. Deviation	12,017	10,953

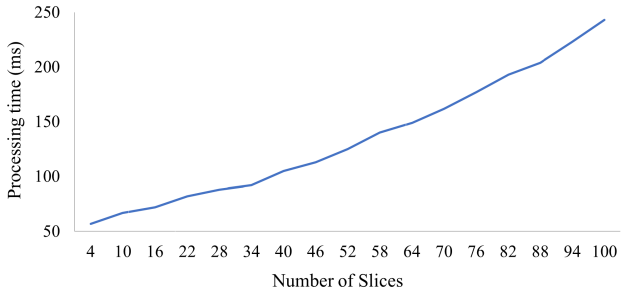

FIGURE 15. Processing time (in milliseconds) over the number of slices using Disc Method.

correlation coefficient equals to 0.9205 and the trendline equation is Estimated Mass = 1.0076 × Estimated Volume − 2330.2. This trendline needs the estimated volume as the input to compute mass of starfruit.

III. RESULTS AND DISCUSSION

The statistical properties of 300 training samples of starfruit which are means, standard deviations, and minimum and maximum values of actual volume (mm^3) and actual mass (mg) for starfruit are shown in Table 1. This study extracts each starfruit into 4−100 slices and validates the performance which are processing time, errors, standard deviation, and correlation coefficient to the actual values then we used paired t-test to compare the difference between our results to the actual volume, and mass.

A. PROCESSING TIME

Figures 15 - 16 show the processing time of the system (from the initial processing of the raw image to the completion of the dimension, volume and mass estimations) using Disc method and Frustum method, respectively. In general, the processing time of both methods is quite similar and linear, they grow with increasing number of slices. At 100th slice, the processing time of Disc Method is 243 milliseconds, and that of the Frustum Method 240 milliseconds. At 4th slice, the processing time of Disc method and Frustum method is 57 milliseconds and 58 milliseconds, respectively. It means the proposed system can estimate the volume and mass of an irregular shape fruit from 4.1 frames per second to 17.5 frames per second depending on the number of slices.

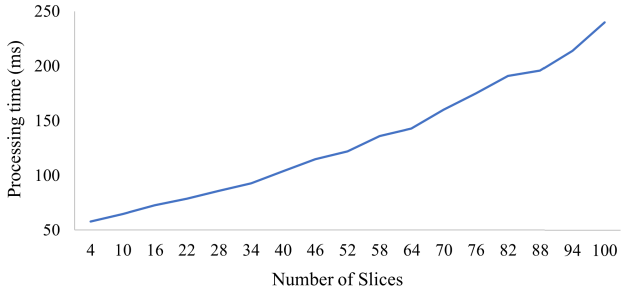

FIGURE 16. Processing time (in milliseconds) over the number of slices using Frustum Method.

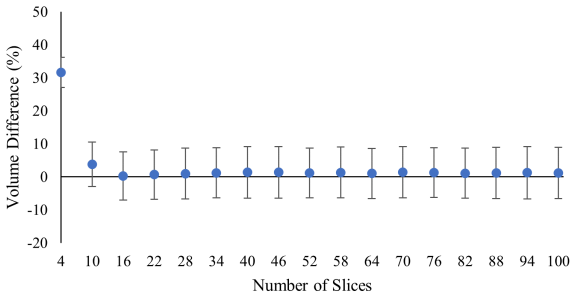

FIGURE 17. Error and standard deviation in estimated volume over the number of slices using Disc Method.

B. VOLUME AND MASS ESTIMATION

For volume estimation, our proposed method responds to the lowest error of 0.23% for the Disc Method (with a standard deviation of 7.2%) at 18th slice and 0.04% for the Frustum Method (with a standard deviation of 7.4%) at 20th slice

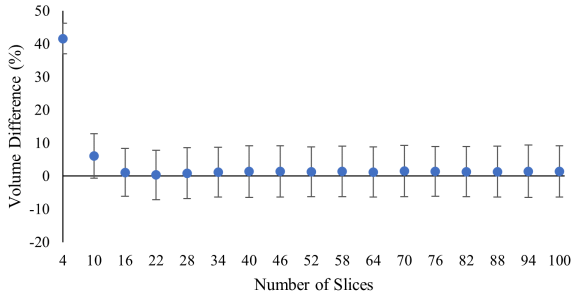

FIGURE 18. Error and standard deviation in estimated volume over the number of slices using Frustum Method.

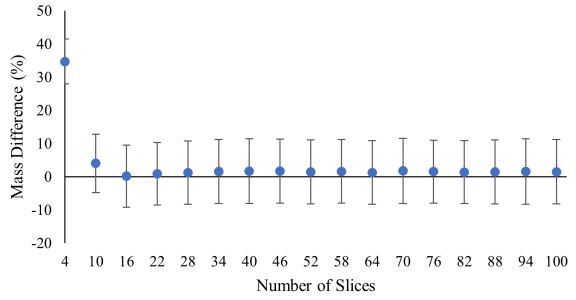

FIGURE 19. Error and standard deviation in estimated mass over the number of slices using Disc Method.

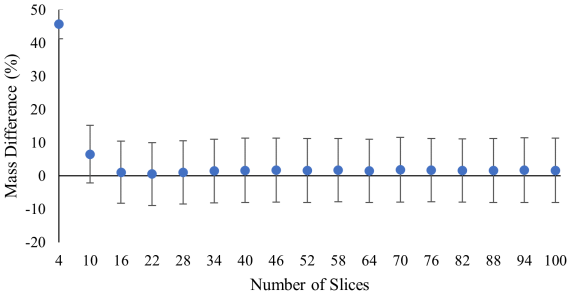

FIGURE 20. Error and standard deviation in estimated mass over the number of slices using Frustum Method.

which are respectively shown in Figure 17 and Figure 18 for volume estimation.

For mass estimation, the lowest error of 0.17% for the Disc Method (with a standard deviation of 9.35%) at 16th slice and 0.21% for the Frustum Method (with a standard deviation 9.36%) at 20th slice which are respectively shown in Figure 19 and Figure 20.

From 20th slices onwards, the results seem to be saturated in around 1.2% error for both volume and mass while its standard deviations are around 7.3% for volume and around 9% for mass.

C. CORRELATION COEFFICIENT VALIDATION

In linear regression, the correlation coefficient (R-Squared) value with range from 0 to 1 shows how the model fits with the actual values. Referred to Figures 21 - 22, the highest correlation between estimated volume and actual

FIGURE 21. Correlation Coefficient (R-Squared) of Disc Method for estimated volume and mass.

FIGURE 22. Correlation Coefficient (R-Squared) of Frustum Method for estimated volume and mass.

volume, estimated mass and actual mass of Disc Method are 0.9695 and 0.9255 while the lowest R-Squared is 0.9472 and 0. 0.9086. For Frustum Method, the highest R-Squared values are 0.969 and 0.9242 for estimated volume and mass, and the lowest R-Squared values are 0.9474 and 0.9089.

D. PAIRED-SAMPLE T-TEST VALIDATION

According to the study of Ross and Willson [38], the paired-sample t-test compares two mean values of two separate groups with the feature that each observed item in one group has a pairwise similarity with an item in the other group. In this study, we used IBM SPSS Statistics software to calculate the parameters between the difference of actual value versus estimated value. For volume comparison in Table 2, the results of Disc Method and Frustum method are validated at 10th slice, 16th slice, 22nd slice, 40th slice and 100th slice to make the results more convincing throughout the number of slices. All the p-values are greater than 0.05 with the different in mean values of actual volume and estimated volume are in the range from -552.67 mm^3 to 746.53 mm^3 for Disc method and from -534.18 mm^3 to 753.19 mm^3 for Frustum method. These parameters prove that our results are not statistically significant at the 5% level.

In Table 3, we similarly validated the difference between actual mass values and estimated mass values of Disc Method and Frustum Method at 10th slice, 16th slice, 22nd slice, 40th slice and 100th slice. The range of different in mean values of Disc method is from -422.22 mg to 691.58 mg and of Frustum method is from -399.92 mg to 710.22 mg. In addition, all the p-values are greater than 0.05 which prove that our results are not statistically significant at the 5% level.

TABLE 2. Paired-sample t-test between actual and estimated volume of Disc Method and Frustum Method.

	Number of slices	Mean (mm^3)	Std. Error Mean	Paired t-test (p-value)	95% Confidence level of mean difference	
					Lower	Upper
Disc Method	10	746.53	474.56	0.117	-187.37	1,680.45
	16	395.80	486.41	0.416	-561.41	1,350.02
	22	-222.34	491.19	0.651	-1,188.98	744.29
	40	-552.67	495.18	0.265	-1,527.17	421.82
	100	-369.45	495.05	0.456	-1,343.68	604.76
Frustum Method	10	753.19	474.91	0.114	-181.39	1,687.79
	16	440.80	484.20	0.363	-512.08	1,393.69
	22	20.01	488.14	0.967	-940.62	980.65
	40	-534.18	494.22	0.281	-1,506.77	438.41
	100	-487.17	497.98	0.329	-1,467.18	492.82

TABLE 3. Paired-sample t-test between actual and estimated mass of Disc Method and Frustum Method.

	Number of slices	Mean (mg)	Std. Error Mean	Paired t-test (p-value)	95% Confidence level of mean difference	
					Lower	Upper
Disc Method	10	691.58	424.22	0.104	-143.25	1,526.43
	16	423.10	431.79	0.328	-426.64	1,272.85
	22	-103.23	435.57	0.813	-960.42	753.94
	40	-422.22	440.20	0.338	-1,288.52	444.08
	100	-310.06	439.24	0.481	-1,174.48	554.34
Frustum Method	10	710.22	423.18	0.094	-122.58	1,543.02
	16	446.03	431.40	0.302	-402.93	1,295.00
	22	91.45	433.90	0.833	-762.44	945.35
	40	-399.92	439.46	0.364	-1,264.75	464.90
	100	-361.28	439.78	0.412	-1,226.76	504.18

E. DISCUSSION

The results of these two methods above are not too different and both have good accuracies and processing time (with 17.5 FPS for 4 slices). The combination of the Disc method (or Frustum method), image processing, machine vision, and geometry is applied not only to starfruit but also to other fruit shapes to estimate the dimension, volume, and mass. In that case, the geometry part needs to be reworked based on the physical properties of the fruit while the rest of the system could be left as is, Tri T. M. Huynh et al. also presented their estimating methods (combination between the Disc method and other methods) which are closely similar to our proposed method for estimating volume and mass of elliptical cross-section fruits such as sweet potatoes [36], carrots and cucumbers [39] with the average width/height ratios are 0.93, 0.9531 and 0.9677, respectively. While their proposed algorithms get the lowest error for estimating Japanese sweet potato, carrot, and cucumber volume are 4.14%, 3.421%, and 3.205%, respectively (with the correlation coefficients are 0.98, 0.9289, and 0.9199, respectively), their mass estimation accuracies are 96% for the Japanese sweet potato, 95% for the carrot and 96.7% for the cucumber. In general, the accuracy of estimating the volume and mass of the fruit depends on the physical shape and its density, the results of Tri T. M. Huynh et al.'s methods and our proposed method have good performance. The combination of the Disc method (or Frustum method) and object slicing method is suitable for estimating volume with high accuracy and low processing time.

Finally, to re-validate the accuracy of our proposed method, 100 new samples (Averrhoa carambola L., pale green in color and various shapes) were collected from supermarkets in Ho Chi Minh City to estimate dimension, volume, and mass. The results do not differ much from the estimations of the first 300 starfruits for both methods, with errors are respectively around 5.12% and 4.84% at 10^{th} slice for volume and mass estimation when applying Disc method, and gradually saturated at 1.28% error (for volume estimation) and 1.42% (for mass estimation) from 20^{th} slice onwards. Similarly, the results of Frustum method are around 5.32% and 5.11% at 10^{th} slice for volume and mass estimation, respectively. The saturated errors are around 1.3% for volume estimation and 1.46% for mass estimation from 20^{th} slice onwards.

IV. CONCLUSION

Our hardware configuration needs only one digital camera built into the top of the frame to take a single top-view image of starfruit to estimate its volume, mass, and dimensions. In this paper, two methodologies (Disc method and Frustum method) use image processing, machine vision, and geometry have been effectively built for quality control evaluation of starfruit which has high nutritional content but has a significant and irregular shape. The following experimental results from 400 samples (including 100 samples for re-validation) indicate that the strategy provides highly competitive outcomes. While the highest accuracy of volume estimation using the Disc method is up to 99.77% at 18^{th}

slice (with the R-squared of 0.9553) and using the Frustum method is up to 99.96% at 20th slice (with the R-squared of 0.9538), the highest estimated mass results achieve 99.83% of accuracy at 16th slice (with the R-squared of 0.9158) when applying Disc method and 99.79% of accuracy at 20th slice (with the R-squared of 0.915) for Frustum method. Other results of volume and mass estimation are also good while the accuracies are over 90% from 10 slices and all the correlation coefficients (R-squared value) are higher than 0.94 for volume estimation and 0.90 for mass estimation. The results of these two methods have good performance and low computing time. So, our approach could be used to design and build industrial weighing or sizing or packaging systems for starfruit due to its simplicity and efficiency. Furthermore, background subtraction and image binarization are the two important sections that decide the accuracy of our algorithms. Thus, the improvement of light conditions and quality of input images are considered for upcoming projects. Moreover, some potential artificial neural networks and feature selection algorithms [40], [41], [42] that use object's diameters, lengths, and slicing methods or using cameras for solving multiple tasks, classifications [5], [43] might be applied to reduce the processing time, error, and standard deviation in future works.

ACKNOWLEDGMENT

The authors thank the Ho Chi Minh City University of Technology (HCMUT), Vietnam National University Ho Chi Minh City for supporting this study.

REFERENCES

[1] R. Carolino, R. Beleboni, A. Pizzo, F. Vecchio, N. Garciacairasco, M. Moysesneto, W. Santos, and J. Coutinhonetto, "Convulsant activity and neurochemical alterations induced by a fraction obtained from fruit *Averrhoa carambola* (Oxalidaceae: Geraniales)," *Neurochem. Int.*, vol. 46, no. 7, pp. 523–531, Jun. 2005.

[2] H. H. Moresco, G. S. Queiroz, M. G. Pizzolatti, and I. M. C. Brighente, "Chemical constituents and evaluation of the toxic and antioxidant activities of *Averrhoa carambola* leaves," *Revista Brasileira Farmacognosia*, vol. 22, no. 2, pp. 319–324, Apr. 2012, doi: 10.1590/S0102-695X2011005000217.

[3] (2021). *Starfruit Global Top Importers and Exporters*. Accessed: May 2023. [Online]. Available: https://www.tridge.com/intelligences/starfruit

[4] N. T. Dang, M.-T. Vo, T.-D. Nguyen, and S. V. T. Dao, "Analysis on mangoes weight estimation problem using neural network," in *Proc. 19th Int. Symp. Commun. Inf. Technol. (ISCIT)*, Sep. 2019, pp. 559–562.

[5] S. V. T. Dao, "Multimodal classification of mangoes," in *Agricultural Robots—Fundamentals and Applications*. London, U.K.: IntechOpen, Jan. 2019, doi: 10.5772/intechopen.81356.

[6] F. Mendoza and J. M. Aguilera, "Application of image analysis for classification of ripening bananas," *J. Food Sci.*, vol. 69, no. 9, pp. E471–E477, May 2006, doi: 10.1111/j.1365-2621.2004.tb09932.x.

[7] B. Emadi, M. H. Abbaspour-Fard, and P. K. D. V. Yarlagadda, "Mechanical properties of melon measured by compression, shear, and cutting modes," *Int. J. Food Properties*, vol. 12, no. 4, pp. 780–790, Jul. 2009.

[8] A. N. Lorestani and A. Tabatabaeefar, "Modelling the mass of kiwi fruit by geometrical attributes," *Int. Agrophys.*, vol. 20, pp. 135–139, Jan. 2006.

[9] A. J. Hall, H. G. McPherson, R. A. Crawford, and N. G. Seager, "Using early-season measurements to estimate fruit volume at harvest in kiwifruit," *New Zealand J. Crop Horticultural Sci.*, vol. 24, no. 4, pp. 379–391, Dec. 1996.

[10] X. Liming and Z. Yanchao, "Automated strawberry grading system based on image processing," *Comput. Electron. Agric.*, vol. 71, pp. S32–S39, Apr. 2010.

[11] A. Terdwongworakul, S. Chaiyapong, B. Jarimopas, and W. Meeklangsaen, "Physical properties of fresh young Thai coconut for maturity sorting," *Biosyst. Eng.*, vol. 103, no. 2, pp. 208–216, Jun. 2009.

[12] M. Clayton, N. D. Amos, N. H. Banks, and R. H. Morton, "Estimation of apple fruit surface area," *New Zealand J. Crop Horticultural Sci.*, vol. 23, pp. 345–349, Jan. 1995.

[13] B. W. Maw, Y.-C. Hung, E. W. Tollner, D. A. Smittle, and B. G. Mullinix, "Technical notes: Physical and mechanical properties of fresh and stored sweet onions," *Trans. ASAE*, vol. 39, no. 2, pp. 633–637, 1996.

[14] P. Artaso and G. López-Nicolás, "Volume estimation of merchandise using multiple range cameras," *Measurement*, vol. 89, pp. 223–238, Jul. 2016, doi: 10.1016/j.measurement.2016.04.005.

[15] J. Siswantoro, A. S. Prabuwono, and A. Abdulah, "Volume measurement of food product with irregular shape using computer vision and Monte Carlo method: A framework," *Proc. Technol.*, vol. 11, pp. 764–770, Jan. 2013.

[16] J. Chopin, H. Laga, and S. J. Miklavcic, "A new method for accurate, high-throughput volume estimation from three 2D projective images," *Int. J. Food Properties*, vol. 20, no. 10, pp. 2344–2357, Oct. 2017, doi: 10.1080/10942912.2016.1236814.

[17] F. Lo, Y. Sun, J. Qiu, and B. Lo, "Food volume estimation based on deep learning view synthesis from a single depth map," *Nutrients*, vol. 10, no. 12, p. 2005, Dec. 2018.

[18] A. Ziaratban, M. Azadbakht, and A. Ghasemnezhad, "Modeling of volume and surface area of apple from their geometric characteristics and artificial neural network," *Int. J. Food Properties*, vol. 20, no. 4, pp. 762–768, Apr. 2017, doi: 10.1080/10942912.2016.1180533.

[19] F. Hahn and S. Sanchez, "Carrot volume evaluation using imaging algorithms," *J. Agricult. Eng. Res.*, vol. 75, no. 3, pp. 243–249, Mar. 2000.

[20] T. Chalidabhongse, P. Yimyam, and P. Sirisomboon, "2D/3D vision-based mango's feature extraction and sorting," in *Proc. 9th Int. Conf. Control, Autom., Robot. Vis.*, Dec. 2006, pp. 1–6, doi: 10.1109/ICARCV.2006.345248.

[21] W. M. Miller, K. Peleg, and P. Briggs, "Automatic density separation for freeze-damaged citrus," *Appl. Eng. Agricult.*, vol. 4, no. 4, pp. 344–348, 1998.

[22] R. D. Tillet, C. M. Onyango, P. F. Davis, and J. A. Merchant, "Image analysis for biological objects," in *Proc. 3rd Int. Conf. Image Process. Appl.*, Warwick, U.K., Jul. 1989, pp. 207–211.

[23] K. A. Forbes and G. M. Tattersfield, "An investigation into the volumetric determination of apples using machine vision techniques," in *Proc. 9th Annu. South Afr. Workshop Pattern Recognit. Weber*, 1998, pp. 55–59.

[24] M. Soltani, R. Alimardani, and M. Omid, "A new mathematical modeling of banana fruit and comparison with actual values of dimensional properties," *Mod. Appl. Sci.*, vol. 4, no. 8, pp. 104–112, Jul. 2010.

[25] T. Y. Wang and S. K. Nguang, "Low cost sensor for volume and surface area computation of axi-symmetric agricultural products," *J. Food Eng.*, vol. 79, no. 3, pp. 870–877, Apr. 2007.

[26] M. Khojastehnazhand, M. Omid, and A. Tabatabaeefar, "Determination of orange volume and surface area using image processing technique," *Int. Agro Phys.*, vol. 23, no. 3, pp. 237–242, 2009.

[27] S. M. Iqbal, A. Gopal, and A. S. V. Sarma, "Volume estimation of apple fruits using image processing," in *Proc. Int. Conf. Image Inf. Process.*, Nov. 2011, pp. 1–10, doi: 10.1109/ICIIP.2011.6108909.

[28] M. Rashidi, M. Gholami, and S. Abbassi, "Cantaloupe volume determination through image processing," *J. Agric. Sci. Technol.*, vol. 11, pp. 623–631, Nov. 2009.

[29] A. B. Koc, "Determination of watermelon volume using ellipsoid approximation and image processing," *Postharvest Biol. Technol.*, vol. 45, no. 3, pp. 366–371, Sep. 2007, doi: 10.1016/j.postharvbio.2007.03.010.

[30] *Image Processing Method to Determine Surface Area and Volume of Axi-symmetric Agricultural Products*. Accessed: Feb. 27, 2021. [Online]. Available: https://www.tandfonline.com/doi/full/10.1081/JFP-120015498

[31] B. Oyefeso and A. O. Raji, "Estimating mass and volume of Nigerian grown sweet and Irish potato tubers using their geometrical attributes," *Adeleke Univ. J. Eng. Technol.*, vol. 1, pp. 123–130, Aug. 2018.

[32] A. Karaus and H. Paul, "Load cells with small nominal load based on strain gauges using thin-film techniques," *Measurement*, vol. 10, no. 3, pp. 133–139, 1992, doi: 10.1016/0263-2241(92)90009-S.

[33] Tacuna Systems. *Types of Load Cells Overview | Transducers and Sensors*. Accessed: Feb. 27, 2021. [Online]. Available: https://tacunasystems.com/knowledge-base/an-overview-of-load-cells/
[34] *C35 AdvancedLine WD Checkweigher*. Accessed: Feb. 27, 2021. [Online]. Available: https://www.mt.com/vn/en/home/products
[35] *2,000 g Checkweigher | A&D Inspection*. Accessed: Feb. 27, 2021. [Online]. Available: https://inspection.andonline.com/product/2000g-checkweigher/3
[36] T. T. M. Huynh, L. Tonthat, and S. V. T. Dao, "A vision-based method to estimate volume and mass of fruit/vegetable: Case study of sweet potato," *Int. J. Food Properties*, vol. 25, no. 1, pp. 717–732, Dec. 2022, doi: 10.1080/10942912.2022.2057528.
[37] G. V. Venkatesh, S. M. Iqbal, A. Gopal, and D. Ganesan, "Estimation of volume and mass of axi-symmetric fruits using image processing technique," *Int. J. Food Properties*, vol. 18, no. 3, pp. 608–626, Mar. 2015, doi: 10.1080/10942912.2013.831444.
[38] A. Ross and V. L. Willson, "Paired samples T-test," in *Basic and Advanced Statistical Tests*, A. Ross and V. L. Willson, Eds. Rotterdam, The Netherlands: SensePublishers, 2017, pp. 17–19.
[39] T. Huynh, L. Tran, and S. Dao, "Real-time size and mass estimation of slender axi-symmetric fruit/vegetable using a single top view image," *Sensors*, vol. 20, no. 18, p. 5406, Sep. 2020, doi: 10.3390/s20185406.
[40] M. T. Le, M. T. Vo, N. T. Pham, and S. V. T. Dao, "Predicting heart failure using a wrapper-based feature selection," *Indonesian J. Electr. Eng. Comput. Sci.*, vol. 21, no. 3, p. 1530, Mar. 2021, doi: 10.11591/ijeecs.v21.i3.pp1530-1539.
[41] T. T. M. Huynh, T. M. Le, L. T. That, L. V. Tran, and S. V. T. Dao, "A two-stage feature selection approach for fruit recognition using camera images with various machine learning classifiers," *IEEE Access*, vol. 10, pp. 132260–132270, 2022, doi: 10.1109/ACCESS.2022.3227712.
[42] T. M. Le, L. V. Tran, and S. V. T. Dao, "A feature selection approach for fall detection using various machine learning classifiers," *IEEE Access*, vol. 9, pp. 115895–115908, 2021, doi: 10.1109/ACCESS.2021.3105581.
[43] T. T. M. Huynh, T.-D. Nguyen, M.-T. Vo, and S. V. T. Dao, "High dynamic range imaging using a 2×2 camera array with polarizing filters," in *Proc. 19th Int. Symp. Commun. Inf. Technol. (ISCIT)*, Sep. 2019, pp. 183–187, doi: 10.1109/ISCIT.2019.8905122.

HIEU M. TRAN received the B.Eng. degree in automation and control engineering from International University, Vietnam National University Ho Chi Minh City, Vietnam, in 2021, where he is currently pursuing the M.Eng. degree in electrical engineering. He is also a Teaching Assistant with International University, Vietnam National University Ho Chi Minh City. His research interest includes artificial intelligence on the edge and deep learning.

KIEN T. PHAM received the B.E. and M.E. degrees in electrical engineering from International University (VNU-HCM), Ho Chi Minh City, Vietnam, in 2011 and 2014, respectively, and the Ph.D. degree in electrical engineering from the University of Rennes 1 and the Institute of Electronics and Telecommunications of Rennes (IETR), Rennes, France. Since 2019, he has been an Assistant Professor with International University, Vietnam National University Ho Chi Minh City. His current research interests include the analysis and design of transmit arrays, reflectarrays, reconfigurable antennas, genetic algorithms for pattern optimization, and embedded AI. He was a co-recipient of the Best Antenna Design and Applications Paper Award during the 13th European Conference on Antennas and Propagation (EuCAP 2019). He served as a Reviewer for the IEEE TRANSACTIONS ON ANTENNAS AND PROPAGATION and the IEEE ANTENNAS AND WIRELESS PROPAGATION LETTERS.

THANH M. VO received the B.Sc. degree from the Posts and Telecommunications Institute of Technology, Ho Chi Minh City, Vietnam, in 2004, and the M.Sc. degree in telecommunications from the Asian Institute of Technology, Bangkok, Thailand, in 2007. Since 2008, he has been a Lecturer with the School of Electrical Engineering, International University, Vietnam National University Ho Chi Minh City, Vietnam. His research interests include embedded system applications, wireless sensor networks, the Internet of Things, image processing, and embedded machine learning.

TAT-HIEN LE was born in 1981. He received the bachelor's degree in naval architecture and marine engineering from the Ho Chi Minh City University of Technology, Vietnam, in 2004, and the M.Sc. and Ph.D. degrees from Pukyong National University, South Korea, in 2006 and 2009, respectively. He is currently an Associate Professor with the Department of Naval Architecture and Marine Engineering, Ho Chi Minh City University of Technology, Vietnam National University Ho Chi Minh City (VNU-HCM), Vietnam. His research interests include modeling, simulation, and optimization techniques.

TRI T. M. HUYNH received the B.Eng. degree in electrical engineering and the M.Sc. degree in electronics engineering, in 2018 and 2021, respectively. He is currently a Laboratory Specialist with the School of Electrical Engineering, International University, Vietnam National University Ho Chi Minh City, Vietnam. His research interests include embedded systems, machine vision, and deep learning.

SON VU TRUONG DAO received the B.Eng. degree in aeronautical engineering, the M.Sc. degree in manufacturing systems and technology, and the Ph.D. degree in sensors technology, in 2004, 2005, and 2010, respectively. From 2006 to 2008, he was with Hylax Ltd., Singapore, designing high-power laser systems. From 2010 to 2012, he was a Postdoctoral Fellow with Kindai University, Japan. From 2012 to 2015, he was a Senior Scientist with Ritsumeikan University, Japan. His research interests include the development of advanced imaging sensors and systems and applied artificial intelligence.